

BIOFOULING CONTROL: A MICROFLUIDIC ASSESSMENT OF PATTERNED SURFACES

Partha Halder

School of Civil, Environmental and Chemical Engineering, RMIT University, Australia
Telephone: +61 3 9925 3381; Fax: +61 3 9925 0138
E-mail: s3317121@student.rmit.edu.au

Muhammed Bhuiyan

School of Civil, Environmental and Chemical Engineering, RMIT University, Australia
Telephone: +61 3 9925 9014; Fax: +61 3 9925 0138
E-mail: muhammed.bhuiyan@rmit.edu.au

Niranjali Jayasuriya

School of Civil, Environmental and Chemical Engineering, RMIT University, Australia
Telephone: +61 3 9925 3795; Fax: +61 3 9925 0138
E-mail: Nira.Jayasuriya@rmit.edu.au

Abstract

Biofouling, by the sessile growth of microorganisms onto submerged surfaces, presents a serious problem for underwater structures. While biofouling can be controlled to various degrees with different patterned surfaces, the underlying mechanisms are still imprecise. Since long researchers are speculating that microtopographies might influence surface-near microfluidic conditions and thus micro-hydrodynamically preventing microorganism settlement. It is therefore very important to identify the microfluidic environment developed on patterned surfaces and its relation with antifouling behavior of those surfaces. This study considered the wall shear stress distribution pattern of microtopographies as a significant aspect of this microfluidic environment. Though the requirement of effective shear stress is quite low for removing microorganisms at their early stage of attachment, still the development of this critical shear stress is limited due to inadequate inertial forces in the viscous dominated sublayer. So in this study, patterned surfaces were analyzed in the perspective of developing critical microfluidic shear stress with specific distribution pattern to inhibit the gregariousness of microorganisms. A shape comparison of patterned surfaces with equivalent roughness geometries was carried out using CFD simulations. Finally, the study pointed out some geometrical features of a patterned surface and related fluid flow conditions to be considered while selecting the surface for biofouling control.

Keywords: biofouling, CFD simulation, patterned surface, microfluidic approach, wall shear stress

1. Introduction

Biofouling, the unwanted growth of microorganisms on submerged surfaces, is a long known problem for hydraulic structures, water vessels, heat exchangers, oceanographic sensors and aquaculture systems. It is a hierarchical process triggered by organic conditioning onto the underwater surfaces. The attachment and growth of micro and sessile organisms lead to biofouling (Callow and Callow 2011). The initial process of biofouling starts at very small scale in the range of μm to nm , or even in the molecular level. Any 'clean' surface in underwater is rapidly conditioned by organic molecules and matter from the aquatic environment (Rosehahn et al. 2010). Afterward the formation of biofilm composed of bacteria and soft fouling unicellular algae, starts within hours. More complex organisms, such as barnacles, mussels, tubeworms, etc populate the surface at a later stage. Commencing on this perspective, underwater surfaces are conditioned in the initial stage of biofouling, and then other organisms settle gradually. The processes continue over the years and remain irrepressible as they can sustain very harsh environments. Biofouling is a classical example of evolution which is being optimized by nature for millions of years since the first life was created in water.

Conventionally the underwater structures are being protected against biofouling by metal based antifouling coatings (Bers and Wahl 2004). The use of antifouling coatings, in particular those containing Copper and Tributyltin (TBT), is posing more ecological concern due to harmful effects and thus led to a mounting interest in developing non-toxic alternatives (according to International Maritime Organization treaty on biocides, 2008, the use of TBT is restricted).

One of the non-toxic approaches of biofouling control is by surface modification, which usually alters the surface chemical composition and morphology (Rosehahn et al. 2010; Baier 2006) or surface topography and roughness (Bers and Wahl 2004; Bhushan and Jung 2011; Petronis et al. 2000; Schumacher 2007). As such this paper investigates fluid dynamic approach to create low-fouling surfaces by altering surface topography and roughness and thus developing a functional microfluidic environment to prevent biofouling.

2. Fluid dynamic approach

This paper reports systematic investigations that were carried out on addressing the microfluidic approach in connection to engineered patterned surfaces for biofouling control.

2.1 Idea of patterned surfaces

Velocity distribution of fluid flow over any submerged surface is not uniform. Near-surface velocity is always lower than free-stream velocity due to the development of a boundary layer. When microorganisms start to grow on submerged surfaces, they are subjected to very low velocity in the laminar viscous sublayer (Figure 1), where a favourable environment for their attachment and growth onto the surface exists. Even very high free-stream velocity does not have much effect on early stage growth because the thickness of the biofilm is only few μm onto the surface (Callow and Callow 2011).

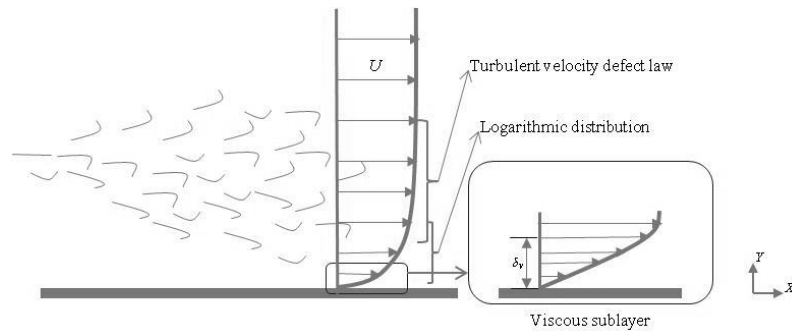


Figure 1: Turbulent boundary layer velocity distribution with laminar viscous sublayer
(reproduced from Crowe et al. 2009)

Here to mention that, this turbulent velocity profile is on smooth surface only. A turbulent velocity profile on fully rough surface merely shows any existence of viscous sublayer. However, for plane surface turbulent boundary layer, a linear distribution of velocity (laminar flow) near the surface exists, where microorganisms attach and subsequently grow. The wall shear stress, τ_w for plane surface is

$$\tau_w = \mu \left. \frac{du}{dy} \right|_{y=0} \quad (1)$$

where μ is dynamic viscosity of water and du/dy is the velocity gradient at $y = 0$. From equation (1), a higher wall shear can be achieved either by increasing viscosity or by increasing steepness of velocity gradient. As viscosity of water is constant for a given temperature and salinity, only higher

free-stream velocity can produce a thinner laminar viscous sublayer. The conventional hydrodynamic approach is based on this concept of ‘the more the free-stream velocity, the less the biofouling’. But it is not feasible to increase free-stream velocity beyond a sensible level to wash away biofouling. According to Finlay et al. (2002), a ship needs to operate at 42 knots (21.4 m/s) to develop an adequate wall shear to remove 4 hours contact *Enteromorpha* spores (325 Pa at a point 30 m from the bow of a ship), whereas the average design speed of bulk cargo ship is about 13.5-15 knots (approx. 7-8 m/s).

Increasing upstream velocity (mean free-stream velocity) is not the only way to develop high shear for a constant viscosity fluid. Generation of disturbance by engineered roughness in laminar sublayer region can be an effective way in this case. Engineered roughness, i.e., patterned or microstructured surfaces essentially increase wall shear stress by increasing frictional velocity, u_* . Frictional velocity can be expressed as

$$u_* = \sqrt{\frac{\tau_w}{\rho}} \quad (2)$$

Here to mention that in any rough surface, wall shear stress increases not only with the viscous effect of fluid (i.e., skin friction), but also with form drag associated with roughness. Surface roughness creates additional drag in comparison to smooth surface in a given fluid flow. So velocity distribution over submerged surface changes according to surface roughness pattern.

In the previous studies with microstructured surfaces, roughness geometries were selected mainly based on biomimetic design. For example, Petronis et al. (2000) considered riblet and pyramid shaped geometry with varying height, base, wall inclination and spacing. Bers and Wahl (2004) mimicked microtopographies from four different marine species whose forms were like spiculed, rippled, ridged and knobbed shaped. In a relatively recent work, Schumacher et al. (2007) designed nano-force gradient Sharklet AFTM where geometric pattern of shark skin (lateral ribs with varying dimensions) was compared with other conventional shapes like ridge, triangles, circular pillars, etc. In all these studies, shape influenced microfluidic analysis were absent, however most of them emphasized on its necessity.

2.2 Development of roughness geometries

For developing a set of comparable geometries based on shape dependent roughness, the individual roughness geometries were created from 8 blocks of constant aspect ratio as shown in Figure 2.

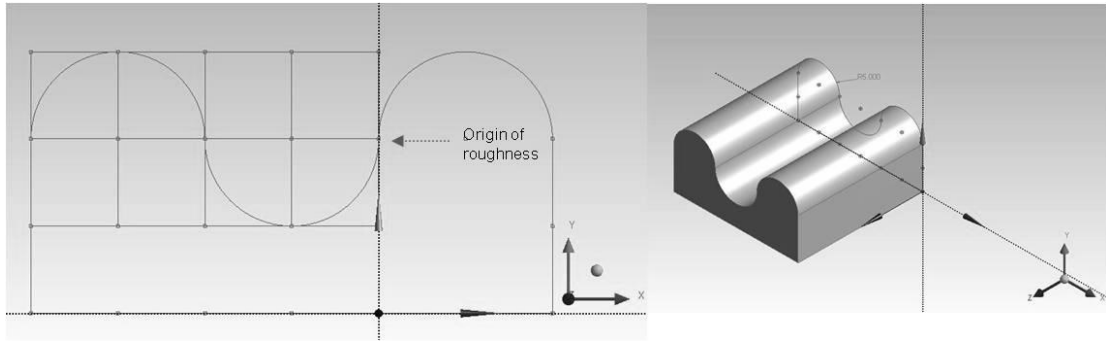


Figure 2: Block approach with constant aspect ratio for a sample geometry (semicircular roughness)

Each block contained a single shape. The second left top block is the mirror image of the first left top block. If the top two blocks were protrusion as in Figure 2, the bottom right two blocks would be depression. The roughness geometry being developed was containing same height of protrusion and depression in succession. Thus it can be considered that the location of virtual origin (ε , the error in origin of roughness) was not changing with roughness geometry and was located at the centre of the total roughness height. Figure 2 is showing roughness development for a semicircular shape. Within each block, unlimited variation of shape can be possible. In this paper, a total of four regular shapes (e.g., rectangular, semicircular, triangular and riblet semicircular) as shown in Figure 3 were considered to generate effectively two-dimensional (2-D) roughness.

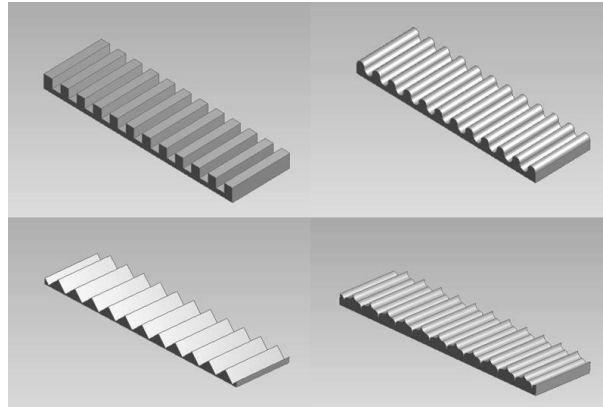


Figure 3: Four different 2-D roughness geometries (rectangular, semicircular, triangular and riblet semicircular)

So for these four geometries, four different rough surfaces were created whose aspect ratio (1:1), roughness height ($10 \mu\text{m}$), spacing ($10 \mu\text{m}$) and the virtual origin ($\varepsilon = 0$) were the same. Perceptibly the equivalent sand grain roughness height, k_s^+ would vary with all these shape geometries. Thus

these patterned surfaces were comparable to each other and with plane surface in the context of origin of roughness. The variation in shear stress due to shape geometries would therefore be comparable to each other. This was the preliminary idea of comparing shape dependent roughness geometries for this study. Hence, in this paper the wall shear distribution was analyzed over these surfaces by using CFD modeling.

3. Fluid domain setup for CFD simulation

Considering the size of microorganism and their attachment to the surface, a zoom in view of the fully developed turbulent flow, very close to the wall of a fluid system was taken to observe the viscous dominated laminar sublayer. It was assumed that the velocity at the top of this viscous sublayer was 0.2 mm/s. This assumption was made based on the calculations in Granhag et al. (2004), where it was stated that to obtain a 0.2 mm/s velocity at 0.01 mm height in the sublayer, a mean velocity of 50 mm/s was necessary at a height of 2.3 mm in the free-stream flow. Thus a *Couette flow* was established with no slip condition in the bottom wall and the given velocity 0.2 mm/s at 0.01 mm height in the sublayer.

The above considered fluid domain (starting from wall surface up to 0.01 mm height) was set for two cases as given below based on fluid domain depth. For both the cases the areal extent of the fluid domain was set at L: 230 μm \times W: 70 μm .

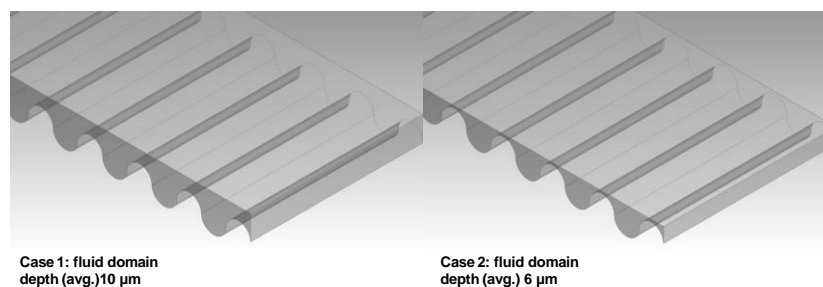


Figure 4: Fluid domain setup for considered two cases

Case 1

The fluid domain depth was not uniform as it was 15 μm at the trough and 5 μm at the crest of the roughness geometry to obtain an average fluid domain depth of 10 μm (see Figure 4). So the virtual roughness origin was considered at 10 μm depth from the fluid domain top surface. Hence from virtual roughness origin the roughness structure protruded 50% height of the total fluid domain.

Case 2

Similarly the fluid domain depth was $11\ \mu\text{m}$ at the trough and $1\ \mu\text{m}$ at the crest of the roughness geometry to obtain an average fluid domain depth of $10\ \mu\text{m}$ (see Figure 4). As a result the virtual roughness origin was considered at $6\ \mu\text{m}$ depth from the fluid domain top surface. Here from virtual roughness origin the roughness structure protruded $\sim 83\%$ height of the total fluid domain.

Fluid velocity for Case 1 at $10\ \mu\text{m}$ height was $0.2\ \text{mm/s}$ and this velocity was set for Case 2 at $6\ \mu\text{m}$ height. So, obviously fluid velocity closer to the surface for Case 2 was higher than that of Case 1. Considering the above situation it can be assumed that the viscous sublayer thickness was reduced in Case 2 than Case 1. The selected fluid domains represented a part of total viscous sub-layer for two different flow conditions.

The water is taken as the fluid. The incompressible Reynolds Average Navier-Stokes (RANS) equations were solved with implicit method to obtain both pressure and velocity fields. Commercially available CFD software *ANSYS CFX* (version 13) was used for the simulation.

4. Results and discussions

The above two cases were compared under four different roughness geometries along with a plane surface for velocity profile and wall shear distribution (see Figures 5-7). The fluid domain setup ensured that free-stream velocity above viscous sublayer is greater for Case 2 than Case 1 as viscous sublayer thickness decreased.

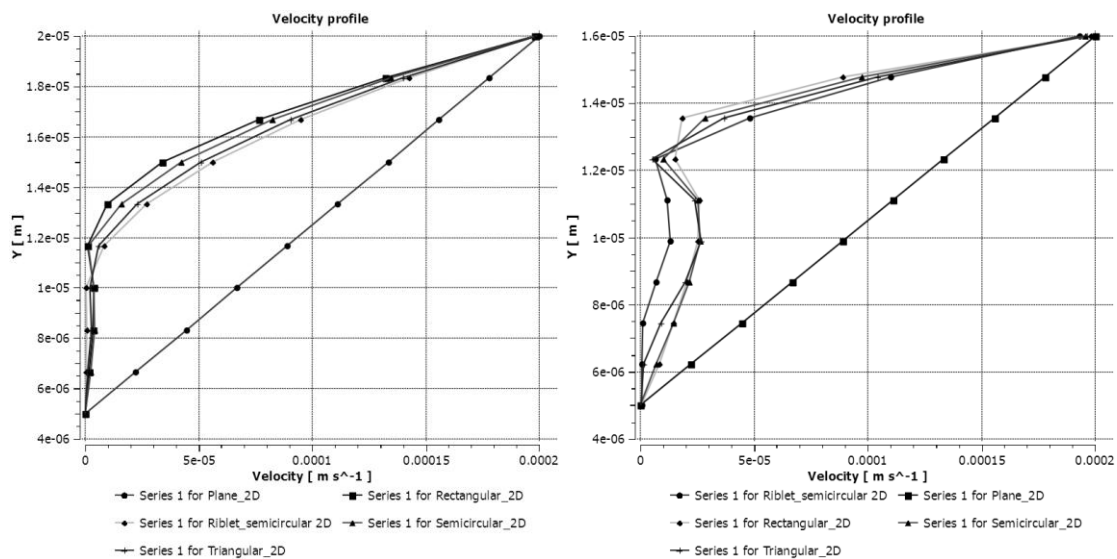


Figure 5: Velocity profile (y-direction) comparison for Case 1 (left) and Case 2 (right)

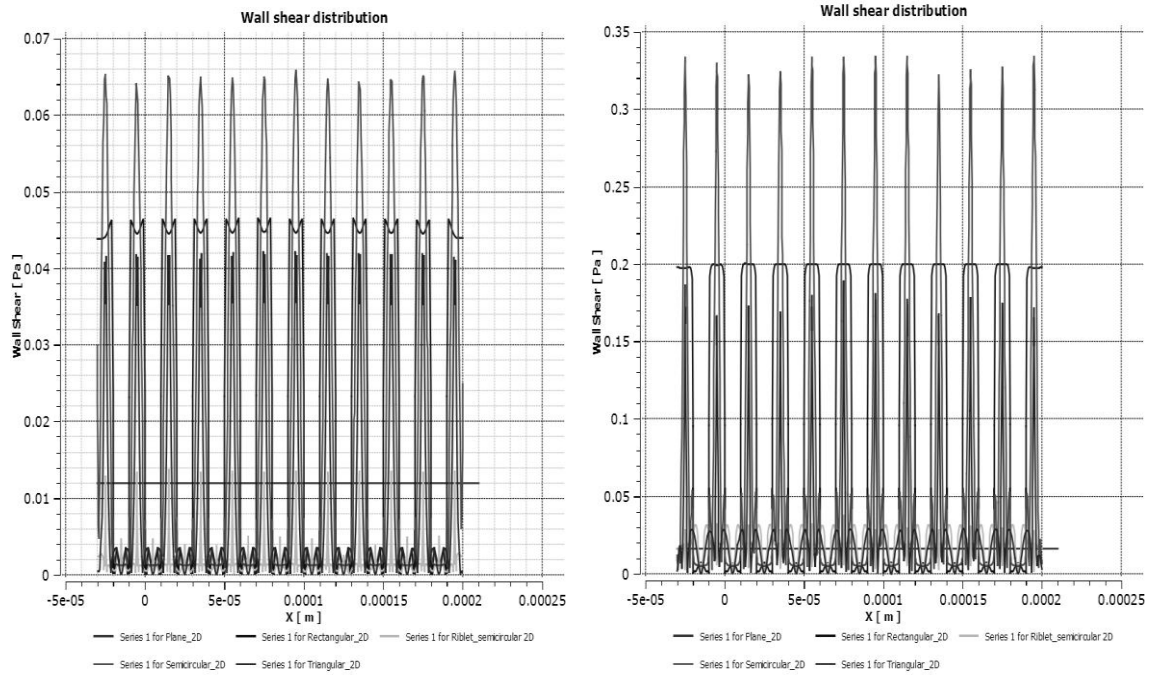


Figure 6: Wall shear comparison for Case 1 (left) and Case 2 (right)

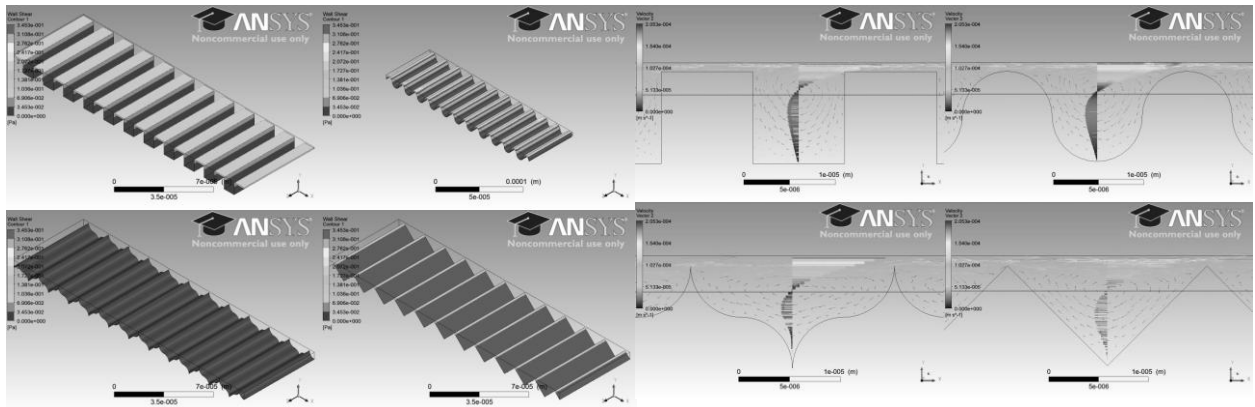


Figure 7: Wall shear distribution in contour map and vortex centre position (Solid straight line at 7.25 μm from bottom wall) for Case 2

It is to note that in Case 2 the viscous sublayer thickness was taken less than Case 1, so the protrusion of roughness geometry was higher in Case 2. As a consequence for every roughness pattern, higher velocity (Figure 5) and higher wall shear stress (Figure 6) were observed in Case 2 than in Case 1. As higher momentum fluid occurs in buffer layer than in linear viscous layer, a better cross mixing was possible in the case of protrusion reaching high momentum zone. A fluctuation in velocity profile was observed in viscous sublayer (Figure 5) due to this cross-mixing of the high momentum fluid.

For every case and roughness geometry, the protruded sections were subjected to higher shear stress than troughs (Figures 6-7). The given roughness geometries were characteristic in distributing the developed wall shear stress. A downward sway of vortex centre as found in riblet semicircular geometry was indicating a better momentum exchange in comparison with other roughness (see Figure 7 and compare with respect to solid straight line at the middle position). A comparatively concentrated wall shear stress at the top surface and sharp edges was observed in rectangle and triangle geometries (see Figure 7). On the other hand, it can be suggested that the semi-circular geometry is more suitable to meet the objective of relatively uniform shear stress distribution over a larger area. This uniform distribution of shear stress is sufficient to dislodge initial attachment of microorganisms over a large area of the surface.

5. Conclusion

Different shape geometries can change drag intensity (increasing or decreasing in comparison with plane surface) for a given velocity (Bechert et al. 2000; Koch and Barthlott 2009; Friedmann 2010). Drag reducing surfaces like shark skin, dimples in golf ball and lotus leaf (Patankar 2004; Bechert et al. 2000) and drag increasing surfaces like non-uniform biofouling at ship hull and pipe-wall (Callow and Callow 2011; Rosehahn et al. 2010; Railkin et al. 2004), are all based on surface roughness geometry and resultant developed flow fields. However, the development of a regular patterned drag distributing rough surface was set as a prime target for biofouling control.

Microstructured surface can contribute in developing high shear stresses near to the wall. Two important points to be noted are: relative roughness height and shear stress distribution. When the roughness height is large enough to protrude in buffer zone (i.e., greater than hydraulically smooth surface) and thus increase the momentum exchange rate, can develop high wall shear stress. Shape of roughness geometry is important in this situation to distribute the shear stress in an effective way for biofouling control.

Microstructured surfaces can inhibit the spreading of colony formation for specific surface pattern under flowing fluid condition. When the high shear developed on patterned surfaces can enclose a zone, it could act as a fence for biofilm growth and its spreading. Thus an arbitrary high shear development in protruded surfaces only would not be an effective solution for biofouling control. An enclosed pattern (e.g., 3D semicircular or dimple pattern) with high shear bounded zone could inhibit the gregariousness of microorganisms (colony size would be smaller) and could be an effective pattern while using a microstructured surface for biofouling control. Moreover, in real situation it is stated that in turbulent flow secondary vortices generate beside the protruded surfaces in the

depression rims (Schlichting 1968; Bechert et al. 2000). These vortices generated lateral flows produce lateral drag and should be considered in 3-D roughness geometry (Friedmann 2010). From this point of view, 3-D roughness surfaces, being symmetric, would produce more lateral drag than 2-D surfaces.

Biofouling control in fluid dynamic approach is a very special case where the conventional method of high velocity fluid is not the appropriate solution. Distribution of a critical shear stress over the entire surface is the prime focus rather than developing a concentrated high shear stress at selected points. This new attempt of surface roughness analysis with shape variation and comparison with equivalent geometries has evolved the microfluidic approach to biofouling control. Thus few optimized surfaces have been identified which can go through further verification and validation to fit with real life scenarios.

References

- Baier RE. 2006. Surface behaviour of biomaterials: The theta surface for biocompatibility. *J Mater Sci: Mater Med* (17):1057-1062.
- Bechert DW, Bruse M, Hage W, Meyer R. 2000. Fluid Mechanics of biological surfaces and their technological application. Springer-Verlag 87:157-171.
- Bechert DW, Bruse M, Hage W. 2000. Experiments with three dimensional riblets as an idealized model of shark skin. Springer-Verlag 28:403-412.
- Bers AV, Wahl M. 2004. The influence of natural surface microtopographies on fouling. *Biofouling* 20:43-51.
- Bhushan B, Jung YC. 2011. Natural and biomimetic artificial surfaces for superhydrophobicity, self-cleaning, low adhesion and drag reduction. *Progress in Materials Science* 56:1-108.
- Callow JA, Callow ME. 2011. Trends in the development of environmentally friendly fouling-resistant marine coatings. *Nature communications* 2:244.
- Crowe CT, Elger DF, Williams BC, Roberson JA. 2009. *Engineering Fluid Mechanics* 9th ed.: John Wiley & Sons Inc.

Finlay JA, Callow ME, Schultz MP, Swain GW. 2002. Adhesion strength of settled spores of the green alga *Enteromorpha*. *Biofouling* 18(4):251-256.

Friedmann E. 2010. The Optimal Shape of Riblets in the Viscous Sublayer. *J math fluid mech* 12:243-265.

Granhag LM, Finlay JA, Jonsson PR, Callow JA, Callow ME. 2004. Roughness-dependent removal of settled spores of the green alga *Ulva* (syn. *Enteromorpha*) exposed to hydrodynamic forces from a water jet. *Biofouling* 20(2):117-122.

Koch K, Barthlott W. 2009. Superhydrophobic and superhydrophilic plant surfaces: an inspiration for biomimetic materials. *Phil Trans R Soc* 367:1487-1509.

Patankar NA. 2004. Mimicking the lotus effect: influence of double roughness and slender pillars. *Langmuir* 20:8209-8213.

Petronis S, Berntsson K, Gold J. 2000. Design and microstructuring of PDMS surfaces for improved marine biofouling resistance. *J Biomater Sci Polymer Edn* 11(10):1051-1072.

Railkin AI. 2004. *Marine Biofouling: colonization processes and defenses* CRC Press.

Rosehahn A, Schilp S, Kreuzer HJ. 2010. The role of "inert" surface chemistry in marine biofouling prevention. *Phys Chem Chem Phys* 12:4275-4286.

Schlichting H. 1968. *Boundary-Layer Theory*. 6th ed.: Mcgraw Hill.

Schumacher JF. 2007. *Control of marine biofouling and medical biofilm formation with engineered topography* University of Florida.